Experimental Techniques (2021) 45:257–271
https://doi.org/10.1007/s40799-021-00441-9

S.I. : COMPUTER VISION AND SCANNING LASER VIBROMETRY METHODS

A Full-Field Non-Contact Thermal Modal Testing Technique Under Ambient Excitation

Y. J. Hu[1] · Z. S. Huang[1] · W. D. Zhu[2] · H. L. Li[1]

Received: 11 May 2020 / Accepted: 12 January 2021 / Published online: 19 February 2021

Abstract
Temperature has significant effects on modal parameters of a structure. However, it is difficult to do a full-field dynamic measurement and identify modal parameters of the structure under high temperature and working conditions. In this work, three-dimensional digital image correlation combined with Bayesian operational modal analysis is used to yield a full-field non-contact thermal modal testing technique under ambient excitation. Thermal modal verification experiments are carried out on a titanium plate with free boundary conditions under ambient excitation by a low-cost high-temperature dynamic measurement system. Natural frequencies and mode shapes of the plate under different average high temperatures are studied in detail. From the experimental process, it is believed that the thermal modal testing technique proposed in this work is an effective alternative testing technique to traditional contact testing techniques, and after some improvements, one can achieve thermal modal analysis of a structure under high temperature and working conditions.

Keywords Thermal modal identification · Dynamic measurement · Ambient excitation · Digital image correlation · Bayesian operational modal analysis

Introduction

Modal analysis is one of the most important experimental techniques to obtain dynamic characteristics of a structure. Thermal modal experimental and analytical techniques under high temperature are of great significance for high-temperature resistant structures in aerospace and nuclear industries. A traditional contact method usually uses experimental modal analysis (EMA) to achieve identification of modal parameters of a structure under high temperature by use of high-temperature resistant accelerometers [1, 2]. However, the effect of additional masses of accelerometers makes the contact experimental method difficult to satisfy requirements for small structures or structures made of lightweight materials under high temperature. It is also difficult for such a contact method to obtain full-field three-dimensional (3D) mode shapes of a structure with a complex surface. A laser Doppler vibrometer (LDV) has been widely used in aerospace engineering and other fields due to its non-contact feature, high accuracy and wide range of measurement frequencies. Especially in recent years, a continuous scanning laser Doppler vibration measurement technology can achieve efficient measurement of operational deflection shapes of a structure through continuous movement of a laser on its surface [3, 4]. With use of a LDV and an impact series excitation approach, structural modal measurements in thermal environments were achieved [5]. However, it is usually necessary to provide single-frequency excitation or mixed-frequency excitation in an experiment for obtaining mode shapes of a structure. It is also difficult to use a LDV on a structure with a large vibration amplitude.

Digital image correlation (DIC) is a full-field, noncontact and remote sensing method in experimental mechanics. Two-dimensional (2D) DIC (2D-DIC) originally developed in the early 1980s needs a series of images of a specimen before and after deformation of a structure [6]. In order to satisfy requirements of 3D deformation measurement on the surface of a structure, Luo et al. [7] proposed a new 3D-DIC method, which has been widely used to measure displacements, stresses and strains of structures in experimental mechanics due to its full-field, noncontact and remote sensing characteristics [8, 9]. Extensive experimental studies using 3D-DIC have been

✉ W. D. Zhu
wzhu@umbc.edu

[1] School of Mechanical Engineering, University of Shanghai for Science and Technology, Shanghai 200093, China

[2] Department of Mechanical Engineering, University of Maryland, Baltimore County, 1000 Hilltop Circle, Baltimore, MD 21250, USA

conducted on static displacements and mechanical characteristics of materials under high temperature [10–14]. With advancement of the performance of high-speed cameras and improvement of the capability of computers, 3D-DIC combined with operational modal analysis (OMA) or EMA is used to identify modal parameters of a structure [15, 16]. However, 3D-DIC has some limitations for modal analysis due to limitations of cameras, such as a low sampling rate and short recording-data length. Bayesian OMA (BOMA) is well suited to do modal analysis to overcome these difficulties. BOMA adopts a Bayesian system identification approach for OMA. Such a method values the traditional fast Fourier transform (FFT) theory as a core and views modal identification as an inference problem in which probability is used as a measure of relative plausibility of outcomes given a model of a structure and measured data central to Bayesian theorem [17]. In particular, the BOMA method is capable of extracting all the information from ambient excitation history data through its posterior statistics and its description method by probability logic better satisfies properties of modal parameters of a structure under ambient excitation. Moreover, it is much more convenient to use BOMA than EMA and conventional OMA due to the following reasons: (1) BOMA can extract modal parameters based only on response measurement and can process response time histories at all measured degrees of freedom (DOFs) of a structure. Only one set of response histories is required [17]. (2) BOMA can directly use noisy measurement without any difficulty and overcome challenges of noisy measurement data and short-length recording data [18, 19]. (3) It obtains not only optimal values of modal parameters, but also uncertainties and signal-to-noise ratios that can be used to evaluate analysis results [19, 20]. Based on the above advantages, Hu et al. [21, 22] presented a novel dynamic modal analysis method that combined 3D-DIC and BOMA. By use of this method, advantages of 3D-DIC and BOMA are integrated, and one can obtain modal parameters of a membrane under ambient excitation and only output vibration of the membrane needs to be measured under ambient excitation.

In a high-temperature environment, the temperature causes changes in physical properties of materials and generate stresses in structures due to factors such as their initial geometrical imperfections, changes in constraints and nonuniform heating on a structure, thereby possibly impacting stiffnesses and vibration characteristics of the structures. Related dynamic experimental studies that ignore influences of the temperature would bring unpredictable consequences. Many researchers used contact or noncontact testing techniques to identify thermal modal parameters [1, 2, 5]. However, due to influence of a high-temperature environment, development of a thermal modal testing technique under working conditions is still a challenging research area. Main difficulties lie in the following aspects: (1) How to apply dynamic loads on a structure under high temperature? The modal identification method based on impact loads is not suitable for identifying modal parameters of the structure under high temperature. (2) How to create high temperature-resistant speckles and verify that

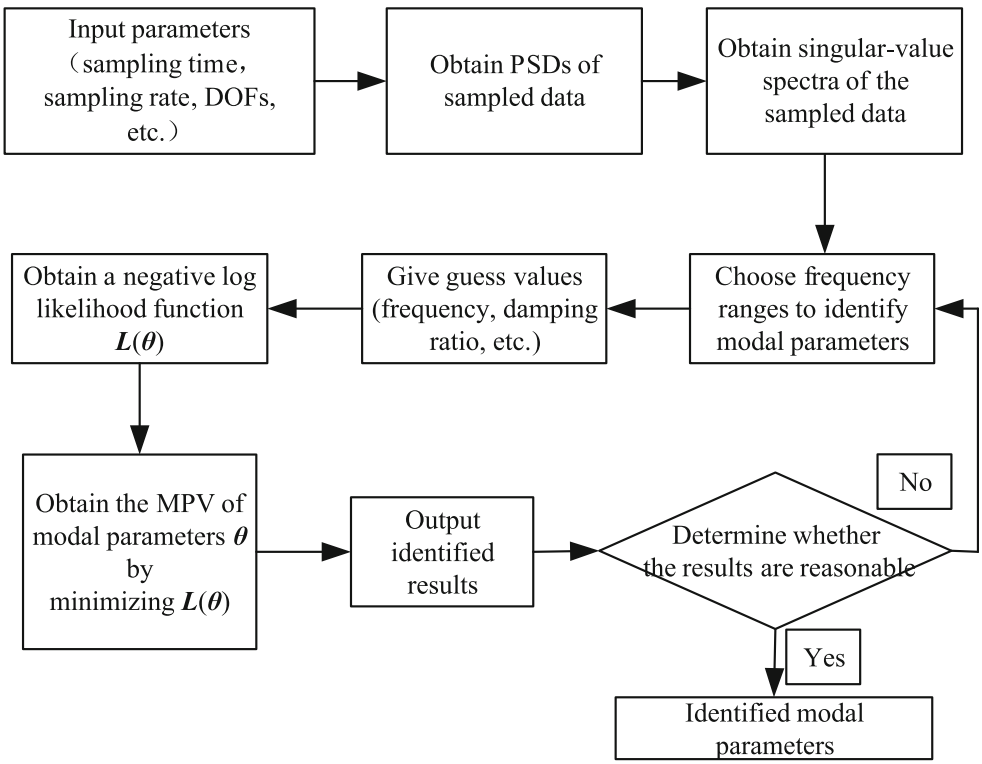

Fig. 1 Flow chart of BOMA

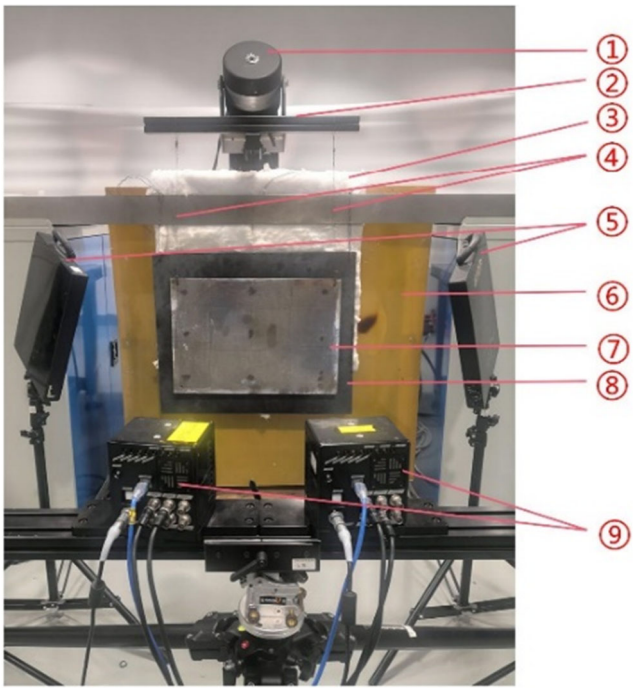

Fig. 2 Dynamic measurement system: ① shaker, ② displacement control platform, ③ high temperature-resistant insulation cottons, ④ copper wires, ⑤ lighting system, ⑥ electromagnetic induction heating device, ⑦ titanium plate, ⑧ iron plate, and ⑨ digital image acquisition system

the method is effective? (3) How to provide a stable temperature field by a low-cost, easily implementable heating method?

In this work, in order to obtain a stable temperature field, a traditional electromagnetic induction heating method has been improved, which can also be used to heat materials that are not sensitive to electromagnetic induction heating. A noncontact testing technique combined 3D-DIC and BOMA is used to achieve identification of thermal modal parameters of a rectangular titanium plate with a small geometrical imperfection and free boundary conditions under different high temperatures and arbitrary excitation. From experimental results, one can find that natural frequencies of the plate with the small geometrical imperfection do not decrease with the temperature. Natural frequencies of the plate first increase and then decrease with the temperature.

Theory

It is difficult to obtain modal parameters of a structure under high temperature due to effects of the temperature and working conditions. A 3D-DIC full-field dynamic measurement method combined with the BOMA method has great advantages in identification of thermal modal parameters of a structure under high temperature because such a method only requires one set of response time histories under arbitrary excitation, and only output vibration of a structure needs to be measured. Using such a non-contact method, one can obtain more vibration data compared with the traditional pointwise measurement method, and achieve full-field dynamic displacement measurement of a structure with complex surfaces.

3D-DIC combines a stereo-vision technique, the triangulation method, and DIC. The surface of a measured structure requires a random speckle pattern on it. By selecting one of the images in the series as a reference image and dividing it into subsets, a correlation algorithm is used on each subset to identify corresponding subsets in all other images of the series. The corresponding subsets are matched by finding peaks of the cross-correlation function or any other correlation metric. The displacement vector is defined by the reference subset and its matched subset in another image so that the displacement distribution map is obtained. During experiments, the surface of a specimen requires a random speckle pattern on it. However, in a high temperature environment, paint particles tend to peel off or burn off. In order to resolve this problem, a laser engraving technology in [11] is used in dynamic experiments in this work. Its most important features are that the size, density, depth and distribution of speckles can be controlled to obtain displacements with high precision, and created speckles can sustain temperatures as high as the melting temperature of the structure.

BOMA directly uses calculated FFTs of measured data without the need of smoothing or averaging the data [19].

(a) (b)

Fig. 3 (**a**) Back of the electromagnetic induction heating device: ① electromagnetic induction heating device, ② electromagnetic coil, and ③ electrical control cabinet; and (**b**) the thermal imager

Table 1 Technical parameters of the laser engraving system

Output power	Galvo scanning velocity	Engraved range	Power stability
20 W	7000 mm/s	100 mm×100 mm	1.2%

One fundamental difference between Bayesian formulation and conventional approaches that has been pointed out by Au et al. [19] is that there are no stochastic averaging and no decision on what average number to use. The analysis process of BOMA is introduced as follows [19, 20]: (1) one obtains measured response data $\boldsymbol{D} = \{\widehat{\boldsymbol{x}}_j \in \mathbb{R}^n : j = 1, \ldots, n\}$ of a structure, such as displacements and accelerations. (2) The FFT is performed on the measured data and an augmented vector $\{\boldsymbol{Z}_k\} = [\boldsymbol{F}_k^T, \boldsymbol{G}_k^T]^T \in \mathbb{R}^{2n}$ that contains real and imaginary parts of the FFT results F_k can be defined, where $\boldsymbol{F}_k^T$ and $\boldsymbol{G}_k^T$ are real and imaginary parts of F_k, respectively. (3) An appropriate frequency bandwidth near a resonant frequency is selected from power spectral density (PSD) results. (4) A negative log likelihood function $\boldsymbol{L}(\boldsymbol{\theta})$ can be obtained as an objective optimization function, where $\boldsymbol{\theta}$ are modal parameters of a structure, including natural frequencies f_i, modal damping ratios ζ_i, mode shapes $\boldsymbol{\Phi}_i$, PSDs of modal forces S_i, PSDs of prediction errors S_{ei}, and signal-to-noise ratios γ_i, where the subscript i denotes parameters with respect to the i-th mode of a structure. (5) Minimizing $\boldsymbol{L}(\boldsymbol{\theta})$, one can obtain the most probable value (MPV) of the modal parameters $\boldsymbol{\theta}$. The flow chart of BOMA is shown in Fig. 1.

Method

High-Temperature Dynamic Measurement System

In order to satisfy requirements of the non-contact dynamic measurement method in a high temperature environment, a low-cost universal dynamic measurement system is designed, as shown in Fig. 2. It consists of five subsystems: (1) an electromagnetic induction heating device, which mainly includes an electrical control cabinet and an electromagnetic coil, as shown in Fig. 3(a). (2) An iron plate is located at about 30 mm away from the surface of the electromagnetic induction heating device. (3) There is a lighting system with multiple white light-emitting-diode illuminators. (4) A displacement control platform can be moved by a stepper motor on it to achieve precise control of the displacement of a measured structure, and the measured structure can be hung on it. (5) There is a digital image acquisition system with two symmetrically placed high-speed cameras with the model Phontron FASTCAM Mini UX50 and two 28 mm/2.8D lens. Traditional electromagnetic induction heating has a fast heating speed; however, it is difficult to control the heating temperature and make the temperature field of the structure stable. In order to resolve this limitation, a composite heating method by combining electromagnetic induction heating and radiant heating is proposed. Such a method can be used to heat materials that are not sensitive to electromagnetic induction heating. The heating process is as follows: (1) the electromagnetic induction heating device is used to heat the iron plate; (2) by use of radiant heating of the iron plate, the titanium plate is subjected to a stable temperature field, where the distance between the iron plate and titanium plate is about 3 mm; and (3) temperature control can be achieved by controlling the output power of the electromagnetic induction heating device. Note that high temperature-resistant insulation cottons with the thickness 30 mm are used to fill the gap between the iron plate and electromagnetic induction heating device and protect the surface of the electromagnetic induction heating device, and a thermal imager of the model FLUKE Ti55FT is

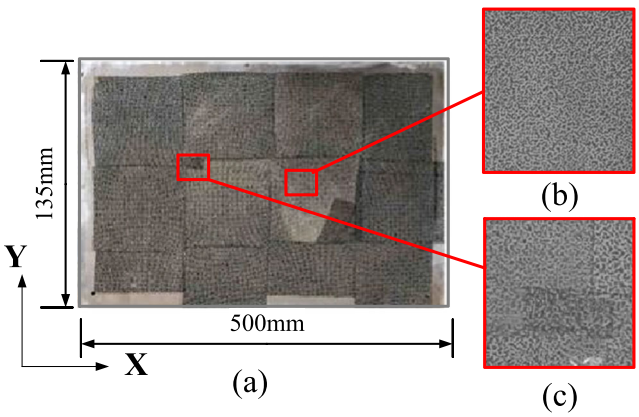

Fig. 4 (**a**) Speckles engraved on the surface of the titanium plate; (**b**) an enlarged view of speckles in a normal region; and (**c**) an enlarged view of speckles at boundaries between two regions

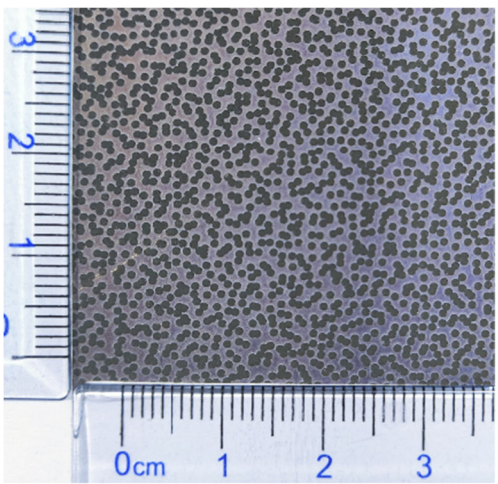

Fig. 5 Size and distribution of speckles

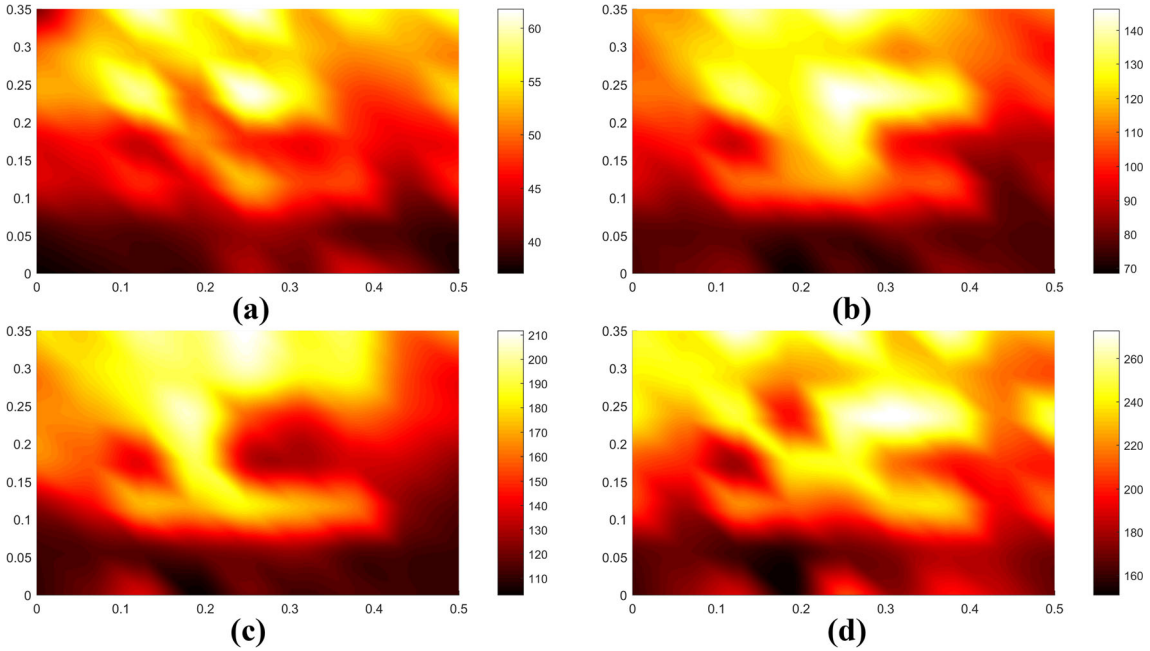

Fig. 6 Distributions of temperatures of the dynamic experiments II ~ V, whose average temperatures are 53.2 °C, 93.5 °C, 142.2 °C and 211.3 °C in (**a**)-(**d**), respectively

used to measure the temperature on the surface of the titanium plate, as shown in Fig. 3(b).

The size of the titanium plate is 500 mm × 350 mm × 2 mm with its mass density being 4.51×10^3 kg/m^3. The titanium plate is hung on the displacement control platform by two very thin high-temperature resistant copper wires, as shown in Fig. 2. With this method, one can simulate free boundary conditions of the titanium plate. In order to simulate random environmental excitation in the laboratory, a shaker with the model hwv-200 is used to provide ambient excitation in the laboratory, which is located near the displacement control platform.

High Temperature Speckles

Accuracies of dynamic measurements based on 3D-DIC with high-speed cameras are closely related to quality of speckles created on the surface of the titanium plate. As mentioned earlier, the laser engraving technology in [11] is used to create speckles and their size, density, depth and distribution can be controlled. Since the speckle pattern is a part of the specimen, it never comes off the specimen surface until reaching the melting temperature of the material. Technical parameters of the laser engraving system is listed in Table 1. In current experiments, the titanium plate is divided into 12 regions to create high temperature speckles since the laser engraving area is not large enough to continuously create the high temperature speckles, as shown in Fig. 4. Distribution of speckles slightly changes at boundaries between two regions due to a random overlap of speckles during their creation, as shown in Fig. 4. The diameter of speckles is about 0.7 mm in this work, as shown in Fig. 5. It can be seen from Fig. 5 that distribution of speckles is random due to a computer generated speckle pattern by random points and the same radius of the speckles used to create the speckle pattern on the surface of the titanium plate [11]. Laser engraving speckles would cause slight damage on shallow surfaces of a measured structure. Average depths of speckles are from 20 μm to 50 μm, which has little effect on measurements of macroscopic mechanical characteristic parameters [11]. However, laser engraving speckles can improve test accuracy of DIC measurements because the size, density, depth and distribution of the speckles can be controlled to suit a particular situation.

Dynamic Experimental Design and Process

The detailed dynamic experimental design and process under high temperature consists of three steps:

Table 2 Measured displacements under different high temperatures and corresponding relative errors

Temp. /°C	30	102	158	197	251
Disp. /mm	−2.68585	−2.71181	−2.70051	−2.70362	−2.71456
Relative error	−0.524%	0.4374%	0.0189%	0.1341%	0.5393%

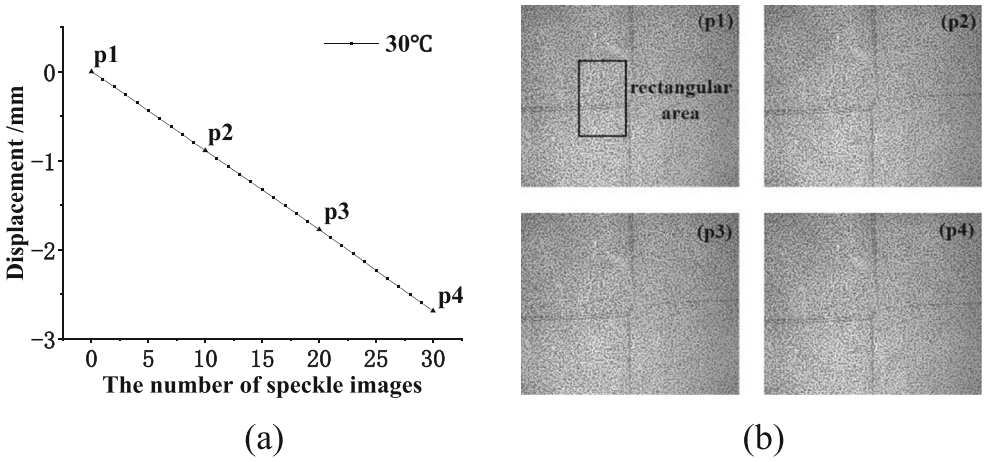

Fig. 7 (**a**) Displacements of the titanium plate at room temperature versus the number of speckle images, and (**b**) speckle images at points p1, p2, p3 and p4

(1) Heating and temperature control. Modal experiments of the titanium plate are designed for five different temperature fields, which include a dynamic experiment I at room temperature, and four dynamic experiments II ~ V under different high temperatures. During the experiments, the electromagnetic induction heating device is used to heat the iron plate, which subsequently heat the titanium plate by heat radiation. In order to obtain a stable thermal environment, when the temperature of the titanium plate reaches the target temperature, a dynamic experiment is started after maintaining this temperature for five minutes. Moreover, one continues to heat the titanium plate and do its dynamic experiment at the next target temperature when the dynamic experiment at the previous temperature is achieved. By continuous dynamic experiments under different temperatures, one can make temperature distribution characteristics of the titanium plate under different temperatures consistent. Temperatures of the titanium plate are measured by the thermal imager. Distributions of temperatures of the four dynamic experiments II ~ V are shown in Fig. 6, whose average temperatures are 53.2 °C, 93.5 °C, 142.2 °C and 211.3 °C, respectively. It is difficult to obtain a uniform

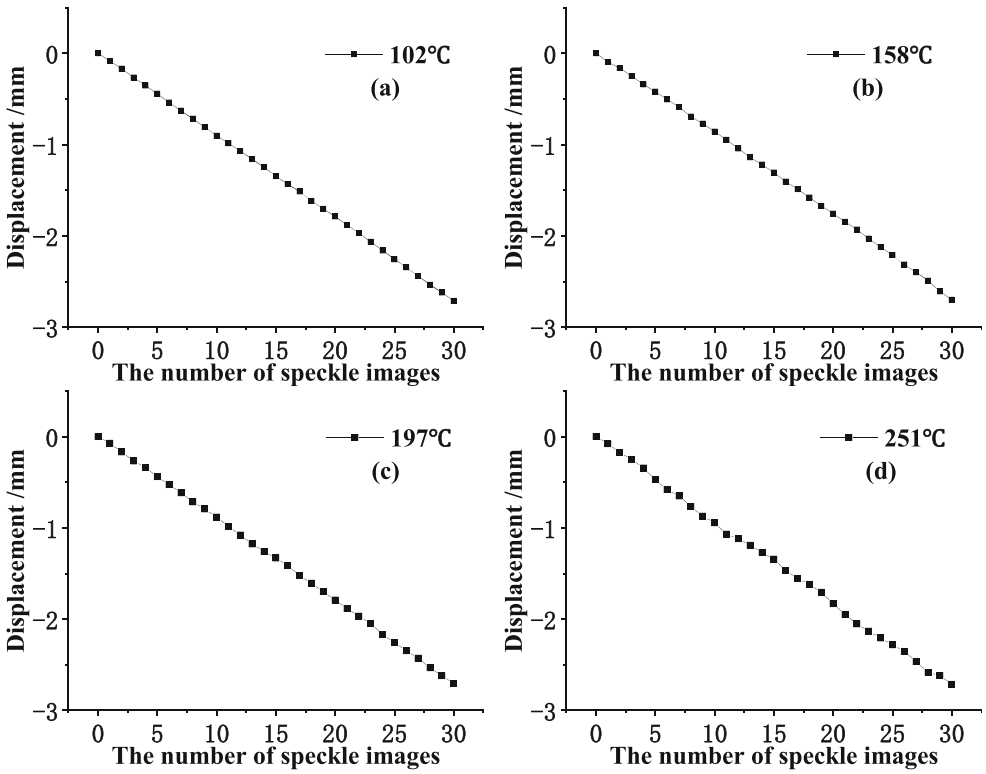

Fig. 8 Displacements of the titanium plate under different high temperatures versus the number of speckle images

Table 3 Identified modal parameters of the titanium plate under different average temperatures

Average temp. /°C	Mode	f /Hz	ζ /%	S_i mm^2/Hz	S_{ei} mm^2/Hz	γ
25.5	1	35.69	0.187	1.25E-05	1.00E-06	1.21E04
	2	46.13	0.090	5.66E-05	2.90E-07	1.89E05
	3	79.88	0.002	1.96E-06	2.55E-07	3.14E04
	4	87.17	0.215	2.47E-06	3.77E-07	1.43E04
53.2	1	37.30	0.260	1.12E-05	1.23E-06	8.37E03
	2	47.28	0.354	9.46E-06	1.23E-06	1.21E04
	3	81.36	0.041	2.97E-07	8.30E-07	1.79E03
	4	87.34	0.235	3.16E-06	2.27E-07	5.78E04
93.5	1	41.70	1.036	5.13E-05	4.37E-07	2.24E04
	2	52.04	1.051	1.56E-04	1.03E-07	2.26E04
	3	85.89	0.166	3.67E-08	1.29E-07	2.36E03
	4	92.46	0.180	6.08E-06	6.55E-08	3.30E05
142.2	1	43.97	0.077	1.13E-05	1.75E-07	8.31E04
	2	55.74	0.392	1.26E-07	4.72E-08	3.92E03
	3	89.01	0.184	3.61E-09	1.42E-08	1.09E03
	4	101.90	0.093	7.01E-08	1.08E-08	5.43E04
211.3	1	37.13	0.553	1.12E-05	1.00E-07	1.53E04
	2	47.07	0.222	4.38E-06	1.04E-07	4.68E04
	3	81.52	0.257	1.01E-06	1.84E-07	2.06E03
	4	87.21	0.002	8.25E-08	7.28E-08	5.82E04

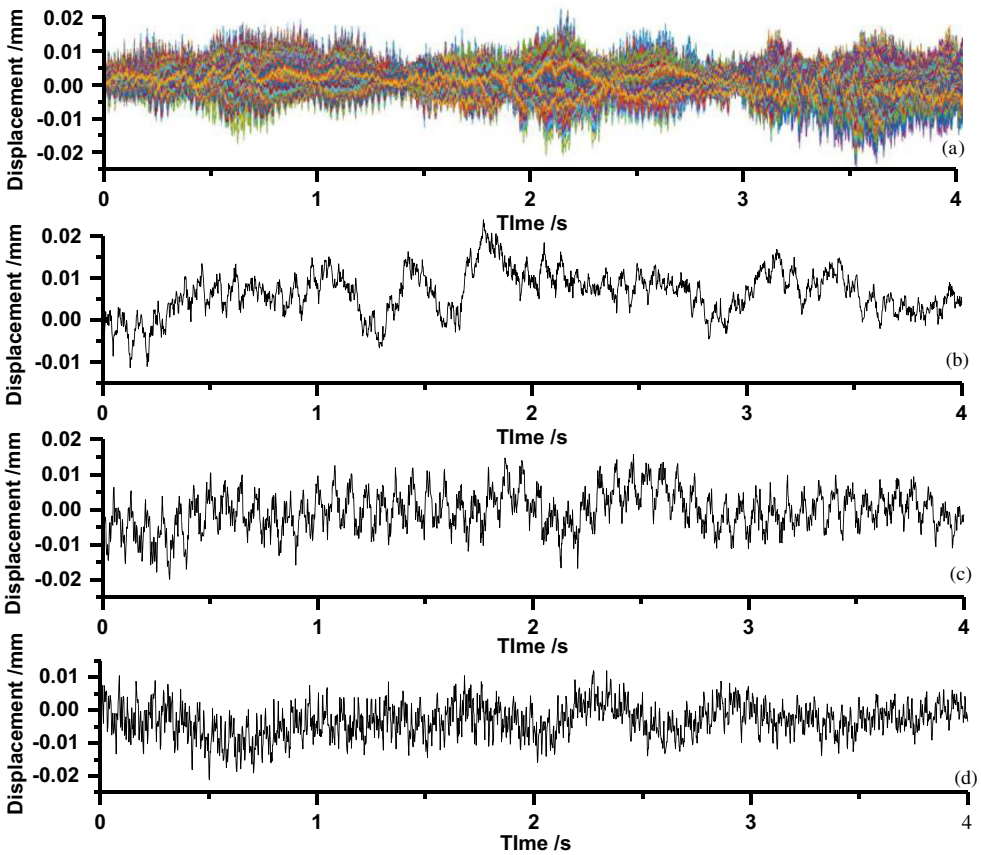

Fig. 9 (**a**) Time-history curves of displacements of all measurement points and (**b**)-(**d**) time-history curves of displacements at points A, B and C of the titanium plate, respectively

temperature field of a plate by a low-cost and easily implementable heating method. Electromagnetic induction heating combined with radiant heating used in this work can yield a stable temperature field of the titanium plate to satisfy the need of dynamic experiments under different high temperatures.

(2) Apply ambient excitation. In order to simulate random environmental excitation in the laboratory, a shaker is used to provide ambient excitation, which is located near the displacement control platform. It is noted that the ambient excitation cannot be too large; otherwise it makes the titanium plate swing back and forth, which affects temperature stability of the titanium plate.

(3) Obtain full-field displacements using 3D-DIC. Two high-speed cameras are located in front of the titanium plate, and each camera has a certain angle with respect to the titanium plate. In this work, the angle between the two cameras is nearly 30°. The measurement distance in this work is about 800 mm, the resolution of the two cameras is 1280 × 1024 pixels, and the sampling rate is 2000 frame/s to ensure that the high-speed cameras can capture a sufficient number of images in a short time duration and obtain accurate displacements of the titanium plate.

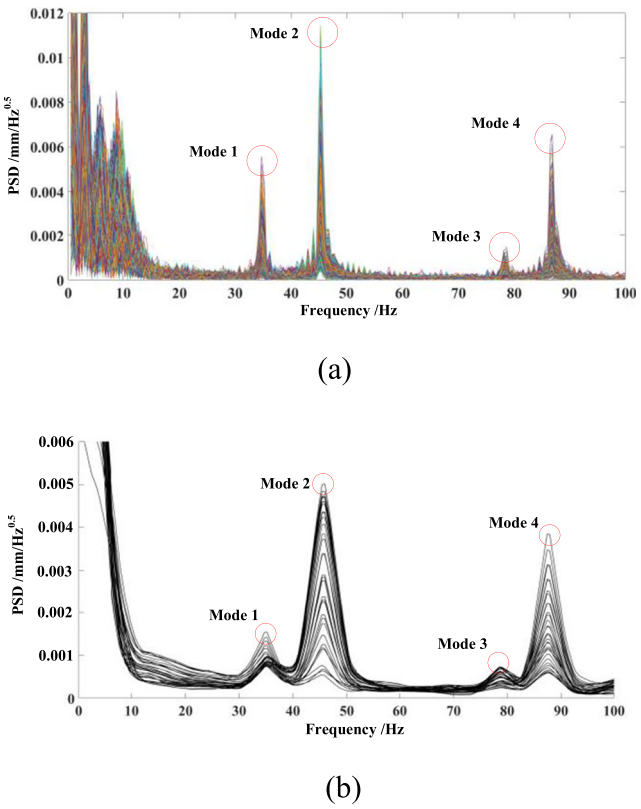

Fig. 10 (**a**) PSDs and (**b**) singular-value spectra from different measurement points of the titanium plate

Experimental Results

The key to the success of a high temperature dynamic experiment lies in the following three aspects: (1) creating high temperature speckles, (2) considering the effect of the thermal gradient on DIC measurements for high temperature applications, and (3) considering radiation effects causing decorrelation issues. Reliability and stability of high temperature laser engraving speckles used in this work were validated in Ref. [11]. The effect of thermal radiation is very small in this work, because there are no changes in speckle patterns when the temperature is below 300 °C. Since thermal radiation would affect speckle patterns under very high temperatures, each camera is equipped with a 532 nm narrow band filter with a bandwidth of 10 nm to block out ambient light and overcome difficulties of radiation from a specimen's surface [11]. In the following section, a rigid body motion experiment is conducted to study the indices of refraction changes in the line-of-site due to thermal gradients. The software used in this work is VIC-3D; a step-by-step guide to conduct DIC tests is outside the scope of this work, and the reader is referred to such resources as the best-practices guide by the International Digital Image Correlation Society [23]. Unless otherwise specified, the subset and step size in this work are 25 and 7, respectively.

Effect of the Thermal Gradient on DIC Measurements

Before the technique to investigate dynamic characteristics of the titanium plate under high temperature is used, the effect of the thermal gradient on DIC measurements for high temperature applications is studied by a rigid body motion displacement of the titanium plate under different high temperatures. Experimental processes are listed as follows:

(1) The titanium plate is hung on the displacement control platform by two very thin high-temperature resistant copper wires.

(2) Let the titanium plate slowly move −2.7 mm by the stepper motor driver on the control platform.

(3) Use the 3D-DIC method to measure displacements of the titanium plate under different high temperatures.

The measurement system is shown in Fig. 2. Two PointGrey GRAS-50S5M-C CCD cameras of 2448 × 2048 pixels and two Schneider Xenoplan 1.9/35 mm lens are used to record speckle patterns. In order to increase measurement

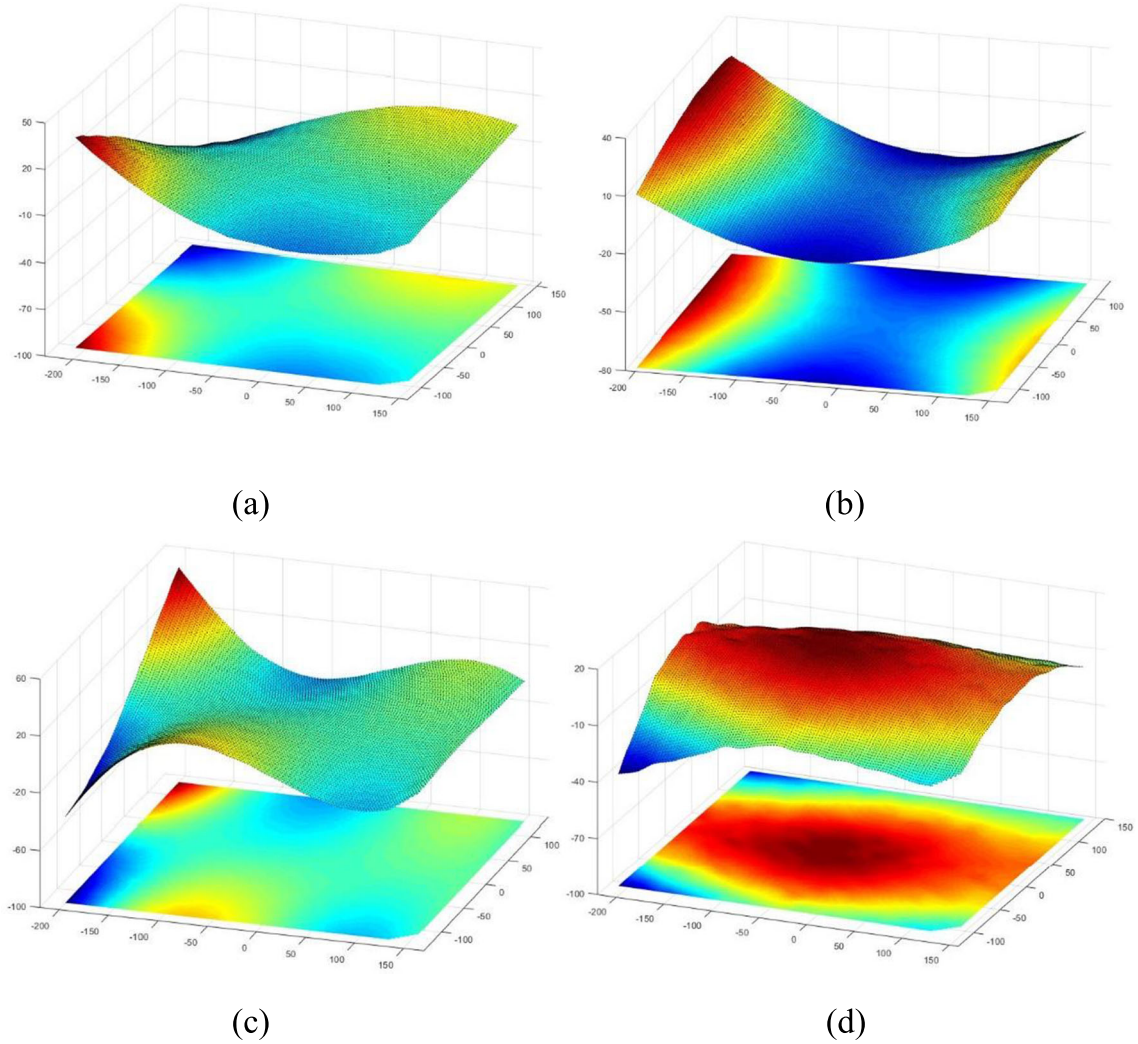

Fig. 11 Mode shapes of the titanium plate at room temperature and their corresponding 2D contours: (**a**) first mode shape, (**b**) second mode shape, (**c**) third mode shape, and (**d**) fourth mode shape

accuracy, 31 speckle images of the titanium plate are recorded during an experiment. Displacements of the titanium plate at room temperature versus the number of speckle images are shown in Fig. 7(a), and speckle patterns at points p1, p2, p3 and p4 as shown in Fig. 7(a) are shown in Fig. 7(b). Note that average displacements in a rectangular area as shown in Fig. 7(b) are used in analyzing displacements of the titanium plate. Displacements under different high temperatures versus the number of speckle images are shown in Fig. 8, where temperatures at midpoints of the titanium plate are obtained by a non-contact infrared thermometer with its accuracy reaching 1%. It can be found from Fig. 8 that displacements under high

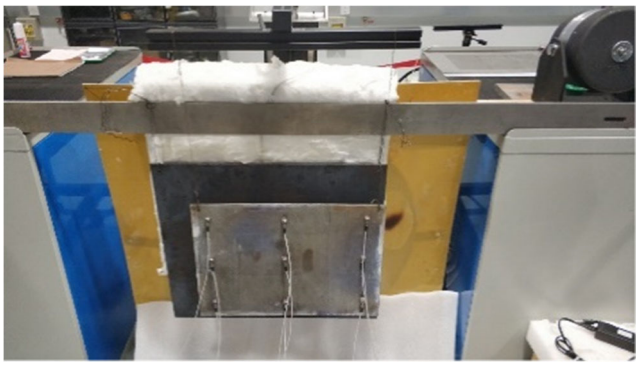

Fig. 12 Experimental setup

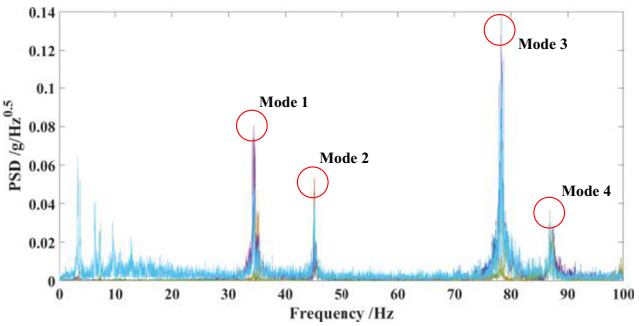

Fig. 13 PSDs from different measurement points obtained by nine accelerometers attached to the titanium plate at room temperature

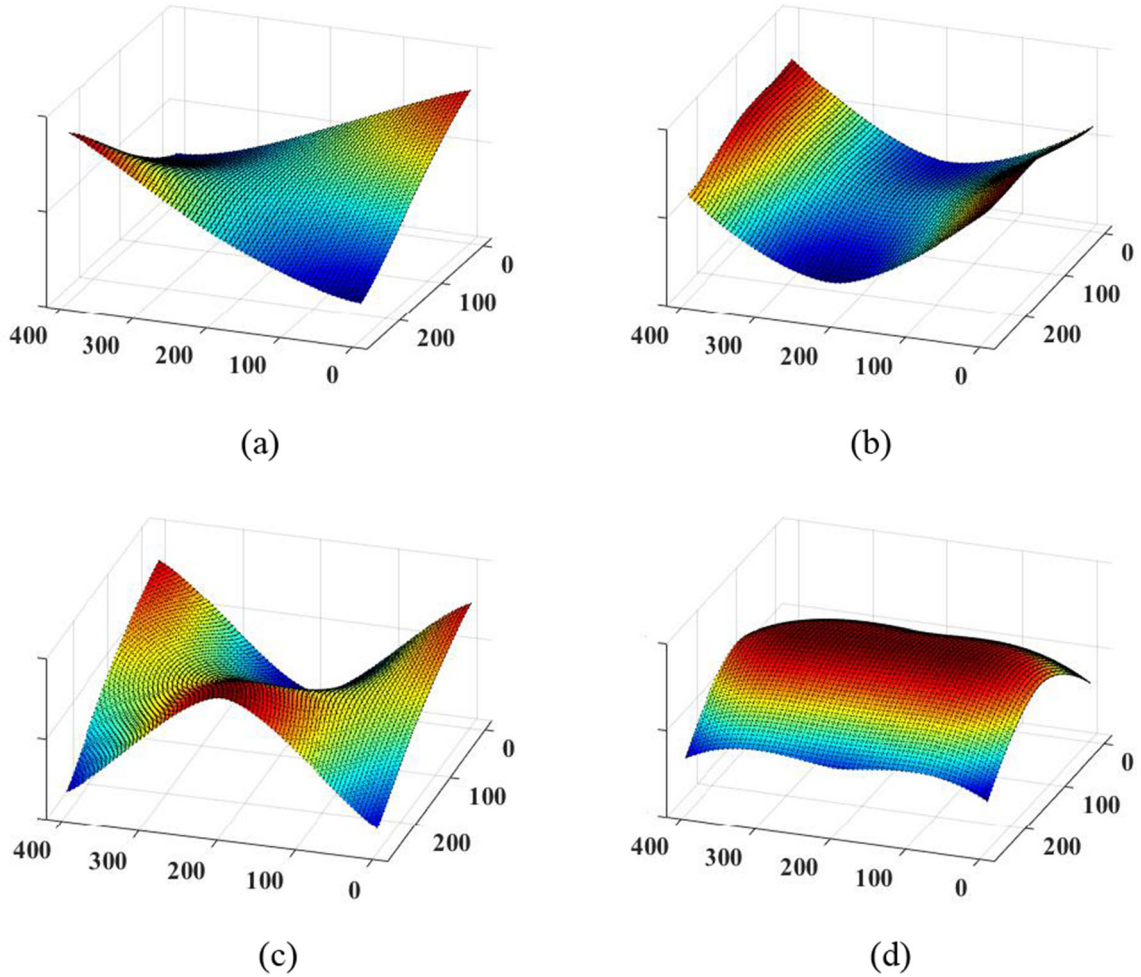

Fig. 14 Mode shapes of the titanium plate at room temperature obtained by accelerometers: (**a**) first mode shape, (**b**) second mode shape, (**c**) third mode shape, and (**d**) fourth mode shape

temperatures have weak oscillations because the heat flow causes the titanium plate to weakly vibrate during the heating process. Measured displacements under different high temperatures and corresponding relative errors are listed in Table 2, where relative error = (measured displacement-2.7)/2.7 × 100%. It can be found from Table 2 that the thermal gradient has little effect on DIC measurements for high temperature applications when the temperature is less than 251 °C.

Modal Identification of the Titanium Plate

Encouraged by the above verification experiment, full-field dynamic displacements of the titanium plate under different high temperatures are obtained by 3D-DIC. The sampling time is one second due to the fact that the maximum storage and sampling rate of the high-speed camera used in this work are 4 GB and 2000 frame/s, respectively. As mentioned above, BOMA can overcome short-length recording data from DIC measurements. In fact, one second of data are enough for identifying modal parameters of the titanium plate. However, in order to increase the accuracy of modal identification, especially for identifying modal damping ratios, experimental data under the same testing conditions and external random excitation are recorded four times. Note that external random excitation in these experiments is controlled by the shaker shown in Fig. 2. Experimental data in the four experiments are combined for modal identification. Time-history curves of out-of-plane displacements of the titanium plate at room temperature at all measurement points and special points A, B and C with coordinates (0.05, 0.31), (0.25,

Table 4 MAC values at different average temperatures

Average temp. /°C	First mode	Second mode	Third mode	Fourth mode
53.2	0.997	0.997	0.990	0.997
93.5	0.995	0.989	0.903	0.968
142.2	0.994	0.985	0.955	0.932
211.3	0.993	0.994	0.958	0.944

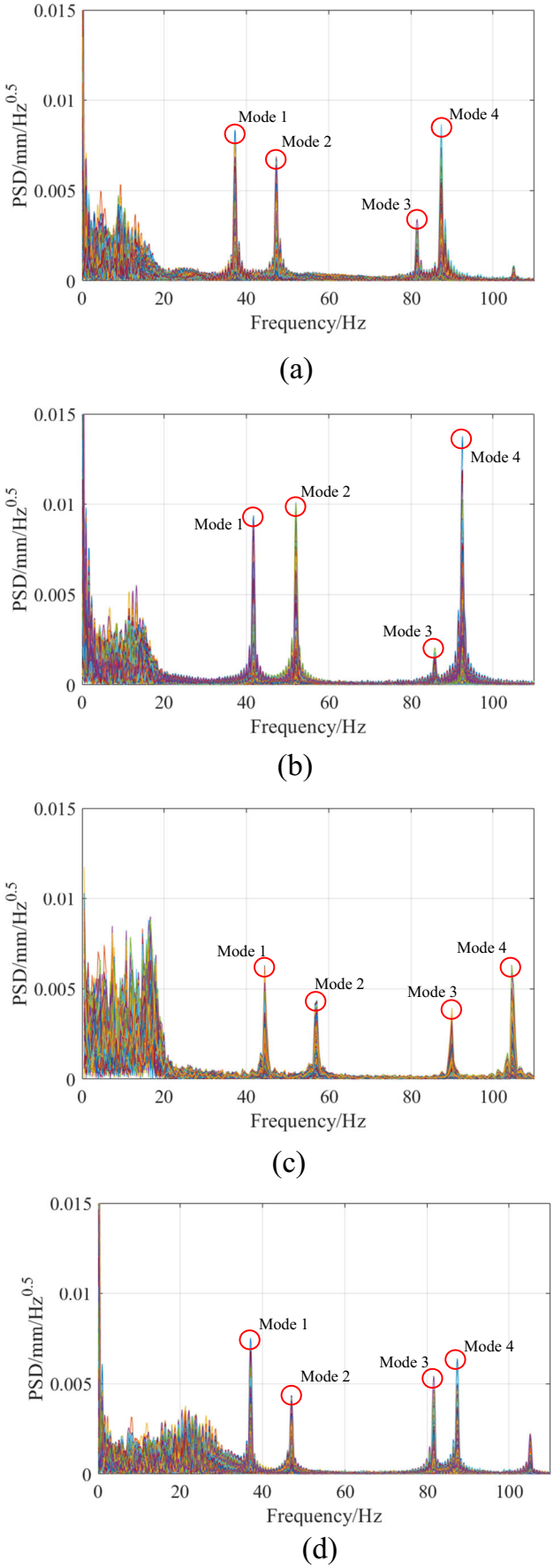

◀ **Fig. 15** PSDs of different measurement points of the titanium plate under different average temperatures: (**a**) 53.2 °C, (**b**) 93.5 °C, (**c**) 142.2 °C, and (**d**) 211.3 °C

0.15) and (0.45, 0.04), respectively, as shown in Fig. 4, are shown in Figs. 9(a)-(d), respectively. One can see that the maximum out-of-plane displacement of the titanium plate is about 0.02 mm. Figures 10(a) and (b) show PSDs and singular-value spectra [24] from different measurement points of the titanium plate in the dynamic experiment I, respectively. Peaks in singular-value spectra can be easily selected, where four peaks can be obviously seen near 35 Hz, 45 Hz, 78 Hz and 97 HZ in the 0 ~ 100 Hz range. Four frequency ranges such as 30 ~ 40 Hz, 40 ~ 50 Hz, 75 ~ 85 Hz and 85 ~ 95 Hz are then used to identify modal parameters of the titanium plate by BOMA at room temperature. Figures 11(a)-(d) show the first four mode shapes of the titanium plate at room temperature and their corresponding 2D contours. Other identified modal parameters at room temperature are listed in Table 3.

In order to validate the accuracy of the above identified results at room temperature, a verification experiment is conducted. An experimental setup with 9 accelerometers with the model Kistler 8763B050BB is shown in Fig. 12.. The titanium plate is hung on the displacement control platform by two very thin high-temperature resistant copper wires, and the sampling rate is 8000 frame/s. PSDs of signals obtained by the accelerometers are shown in Fig. 13. Similar to the above identification process, four frequency ranges of 30 ~ 40 Hz, 40 ~ 50 Hz, 75 ~ 85 Hz and 85 ~ 95 Hz are used to identify modal parameters of the titanium plate by BOMA at room temperature. One can identify that the first four natural frequencies of the titanium plate are 34.8 Hz, 45.1 Hz, 78.2 Hz and 87.0 Hz, respectively. Figures 14(a)-(d) show the first four mode shapes of the titanium plate at room temperature. It can be seen that modal parameters of the titanium plate at room temperature obtained by the accelerometers are consistent with results obtained by the non-contact method in Fig. 11. Note that slight differences between these results in Table 2 are due to additional masses of accelerometers. Hence, the method in this work is would be effective and correct with the verification experiment of the titanium plate at room temperature.

PSDs of different measurement points of the titanium plate in the dynamic experiments II-V are shown in Figs. 15(a)-(e), where the average temperatures are 53.2 °C, 93.5 °C, 142.2 °C and 211.3 °C, respectively. Similar to the above processing method, frequency ranges are selected near peak values of the PSDs to identify modal parameters under high temperature by BOMA. Changes of natural frequencies of the titanium plate versus the average temperatures are shown in Fig. 16, respectively. Relative errors of the first four natural frequencies of the titanium plate at high and room temperatures are shown in Fig. 17, where relative error= $\left(f_i^H - f_i^R\right) / f_i^R \times 100\%$, in

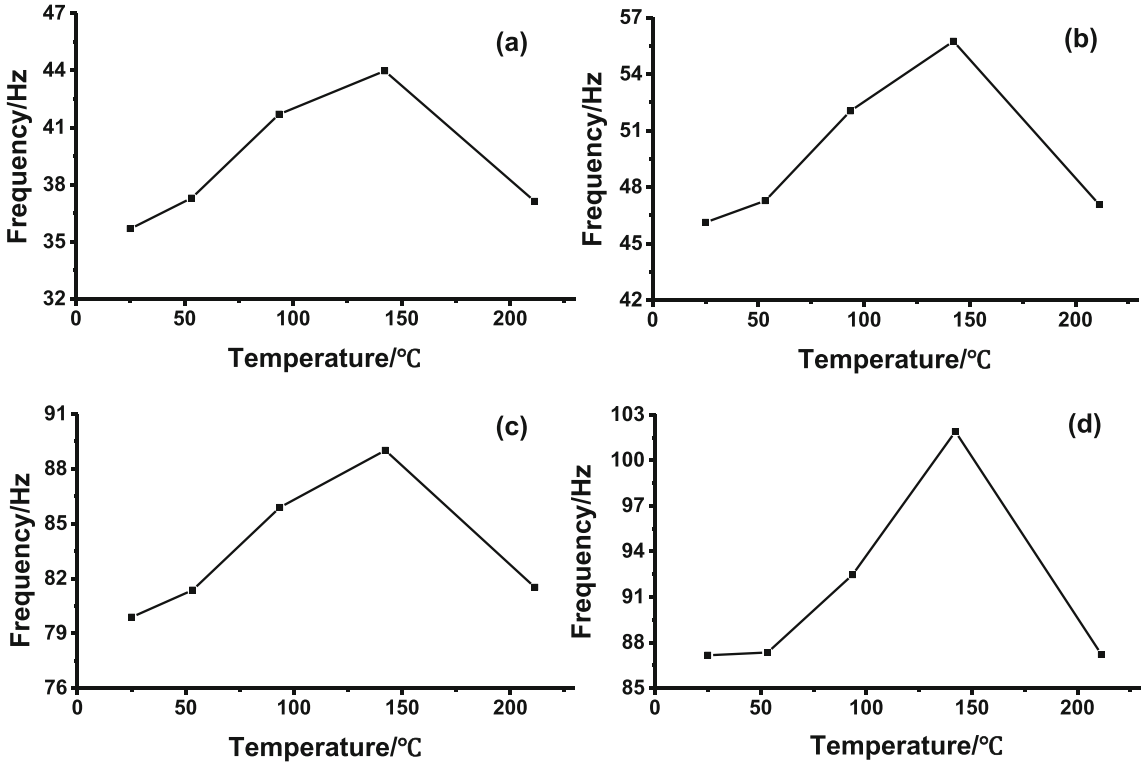

Fig. 16 Natural frequencies of the titanium plate versus the average temperatures, where (**a**)-(**d**) are the first four natural frequencies of the plate, respectively

which f_i^H and f_i^R are natural frequencies of the titanium plate at high and room temperatures, respectively, and the subscript $i = 1,2,3,4$ denotes the i-th mode of the titanium plate. From experimental results, one can find that the first four natural frequencies of the plate do not monotonically decrease with the temperature; they first increase and then decrease with the temperature. This is the case possibly due to a nonuniform temperature field and geometrical imperfection of the titanium plate. It is noted that there was a small geometrical imperfection in the plate, which was a slight bending deformation along to the long side of the plate, and the maximum deformation was close to 1 mm. The effects of a nonuniform temperature field and geometrical imperfection on natural frequencies of the plate under high temperature would be carried out in some further theoretical research. Identified modal parameters under different average temperatures are listed in Table 3. The first fourth mode shapes of the titanium plate of the dynamic experiment V with the average temperature 211.3 °C are shown in Fig. 18. In order to evaluate the effect of the temperature on mode shapes of the titanium plate, the modal assurance criterion (MAC) [25] is used: $\mathrm{MAC} = |\boldsymbol{\varphi}^T \widehat{\boldsymbol{\varphi}}| / (\|\boldsymbol{\varphi}\| \, \|\widehat{\boldsymbol{\varphi}}\|)$, where $\widehat{\boldsymbol{\varphi}}$ and $\boldsymbol{\varphi}$ are mode shapes at high and room temperatures, respectively. MAC values at different average temperatures are listed in Table 4. It can be seen that the MAC values are from 0.90–0.99, which indicates that the temperature has little effect on mode shapes of the titanium plate with free boundary conditions. Comparing MAC values of the first four modes, one can find that high temperature has a relatively large effect on the third and fourth mode shapes, while the first and second modes are little affected.

Discussion

This work is a beginning of high-temperature thermal modal experiments with use of 3D-DIC combined with BOMA. The purpose of this work is to verify the effectiveness of the

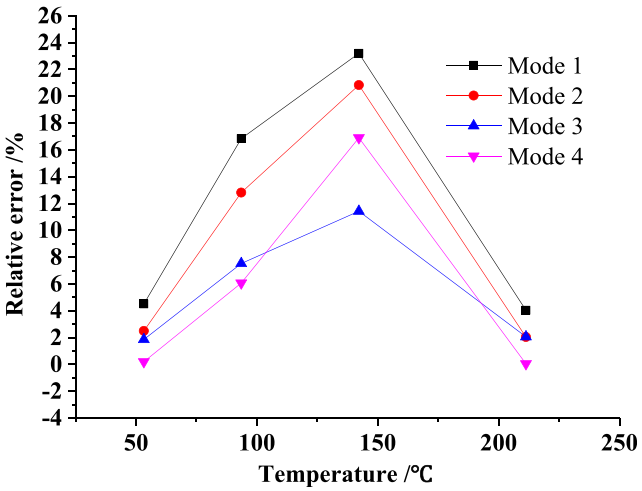

Fig. 17 Relative errors of the first four natural frequencies of the titanium plate at high and room temperatures

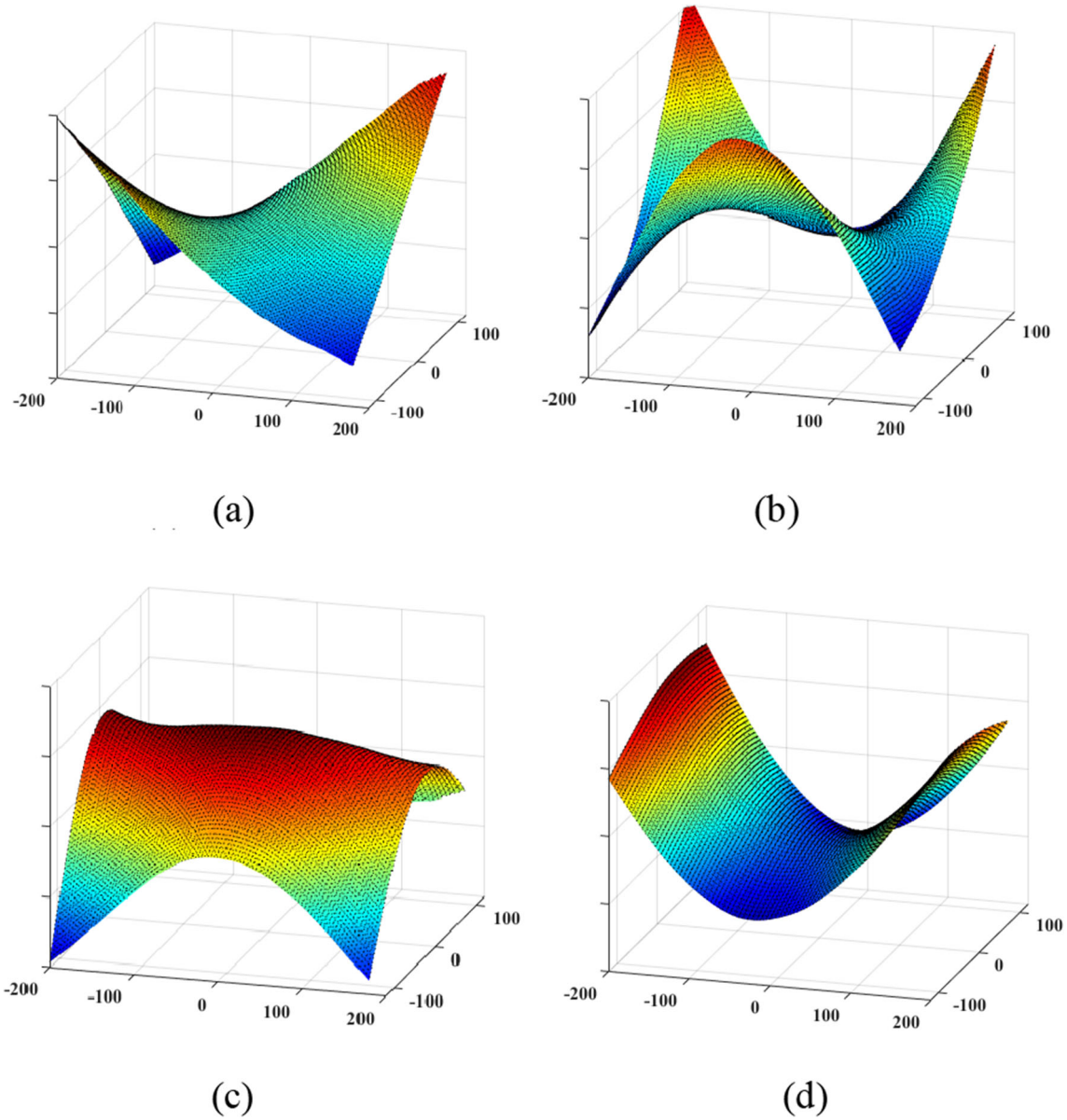

Fig. 18 Mode shapes of the titanium plate of the dynamic experiment V with the average temperature 211.3 ° C: (**a**) first mode shape, (**b**) second mode shape, (**c**) third mode shape, and (**d**) fourth mode shape

experimental technique in high-temperature thermal modal experiments. However, there are still some difficulties in the study of thermal modal identification of a structure:

(1) Heating and temperature control. The heating system in this work has low heat utilization efficiency; thus an insulation chamber can be added to improve the heating efficiency. It is also difficult to obtain a uniform temperature field of the titanium plate with the size of 500 mm × 350 mm × 2 mm. In this work, the maximum relative temperature fluctuation is less than 15% when the area of the titanium plate is $\Gamma_0 : \{(X, Y) | X \in [0.1\ \text{cm}, 0.4\ \text{cm}], Y \in [0.2\ \text{cm}, 0.35\ \text{cm}]\}$, where the maximum relative temperature fluctuation is defined as $(T_{\max} - T_{\min})/T_{avg} \times 100\%$, in which $T_{\max}$, $T_{\min}$ and T_{avg} are maximum, minimum and average temperatures in an area, respectively. The temperature field in the other area of the plate is less uniform than that in Γ_0, but it is stable and can satisfy the need of high-temperature dynamic testing. A more uniform temperature field in thermal modal experiments can be provided by a more controllable heating system.

(2) Effect of the thermal gradient on DIC measurements. The effect of the thermal gradient on DIC measurements for high temperature applications is studied in this work by a rigid body motion displacement of the titanium plate when the average temperature is less than 251 °C. The effect of the thermal gradient on DIC measurements for

higher temperatures needs to be studied. Developing techniques to reduce and compensate for the effect of the thermal gradient on DIC measurements is still a challenging task.

(3) Random reliability of a thermal modal experiment. Relative to modal experiments at room temperature, there are many random factors that can affect random reliability of thermal modal experiments, including quality of a high-contrast speckle pattern under high temperature, temperature field of a structure, testing system and method, initial geometrical imperfection, and so on. One needs to carry out quantitative evaluation of random reliability of a thermal modal experiment.

Conclusions

A full-field non-contact thermal modal testing technique under ambient excitation that combines 3D-DIC and BOMA is proposed in this work. Thermal modal experiments are carried out on a titanium plate with free boundary conditions under ambient excitations by a low-cost high-temperature dynamic measurement system. Experimental results are shown to assess its validity and effectiveness. Four key problems have been addressed for the thermal modal experiments:

(1) The thermal modal testing technique under ambient excitation that combines 3D-DIC and BOMA has two main advantages: easy operation during an experiment, and it has a seemingly high potential as an alternative to do thermal modal analysis of a structure with complex high-precision surfaces under extreme working conditions because it is a noncontact test method and can be used under ambient excitation without human participation.

(2) Laser engraved speckles are first used in dynamic testing under high temperature; the effect of the thermal gradient on DIC for high temperature applications is addressed in this work by use of a rigid body motion displacement of the titanium plate under different temperatures. It is believed that the laser engraving technology would be effective in high-temperature thermal modal experiments under higher temperature.

(3) A stable temperature field is obtained by a low-cost, easily implementable heating method that combines electromagnetic induction heating and radiant heating, which can meet the need of dynamic testing under high temperature.

(4) Some interesting experimental results were obtained. Measured natural frequencies of the titanium plate do not monotonically decrease with the temperature, possibly due to geometrical imperfection of the plate and a nonuniform temperature field. They first increase and then decrease with the temperature. More detailed theoretical research on thermal modal analysis of a plate with geometric imperfection should be carried out to explain this phenomenon.

Acknowledgements The authors would like to thank the financial support from the National Science Foundation (Award No. 1763024), and National Natural Science Foundation of China (Award Nos. 11772100 and 51975379).

References

1. Brown AM (2002) Temperature-dependent modal test/analysis correlation of X-34 fastrac composite rocket nozzle. J Propuls Power 18(2):284–288
2. Bai YH, Yu KP, Zhao J, Zhao R (2018) Experimental and simulation investigation of temperature effects on modal characteristics of composite honeycomb structure. Compos Struct 201:816–827
3. Chen DM, Xu YF, Zhu WD (2016) Damage identification of beams using a continuously scanning laser Doppler vibrometer system. J Vib Acoust 138(5):051011
4. Chen DM, Xu YF, Zhu WD (2019) A comprehensive study on detection of hidden delamination damage in a composite plate using curvatures of operating deflection shapes. J Nondestruct Eval 38:54
5. Bai Y, Yu K, Zhao R, Zhou H (2018) Impact series shaker excitation approach for structural modal testing in thermal environments. Exp Tech 42:429–438
6. Bruck HA, McNeill SR, Sutton MA, Peters WH (1989) Digital image correlation using Newton-Raphson method of partial differential correction. Exp Mech 29(3):261–267
7. Luo PF, Chao YJ, Sutton MA (1994) Application of stereo vision to three-dimensional deformation analyses in fracture experiments. Opt Eng 33(3):981–991
8. Pan B, Qian K, Xie H, Asundi A (2009) Two-dimensional digital image correlation for in-plane displacement and strain measurement: a review. Meas Sci Technol 20:6
9. Reu P (2015) DIC: a revolution in experimental mechanics. Exp Tech 39(6):1–2
10. Chen X, Xu N, Yang LX, Xiang D (2012) High temperature displacement and strain measurement using a monochromatic light illuminated stereo digital image correlation system. Meas Sci Technol 23(12):125603
11. Hu YJ, Wang YJ, Chen JB, Zhu JM (2018) A new method of creating high-temperature speckle patterns and its application in the determination of the high-temperature mechanical properties of metals. Exp Tech 42:523–532
12. Grant BMB, Stone HJ, Withers PJ, Preuss M (2009) High-temperature strain field measurement using digital image correlation. J Strain Anal Eng Des 44(4):263–271
13. Pan B, Wu D, Wang Z, Xia Y (2011) High-temperature digital image correlation method for full-field deformation measurement at 1200 °C. Meas Sci Technol 22(1):015701
14. Berke RB, Lambros J (2014) Ultraviolet digital image correlation (UV-DIC) for high temperature applications. Rev Sci Instrum 85(4):045121
15. Helfrick MN, Niezrecki C, Avitabile P, Schmidt T (2011) 3D digital image correlation methods for full-field vibration measurement. Mech Syst Signal Process 25:917–927
16. Santos Silva AC, Sebastian CM, Lambros J, Patterson EA (2019) High temperature modal analysis of a non-uniformly heated rectangular plate: experiments and simulations. J Sound Vib 443:397–410

17. Yuen KV, Katafygiotis LS (2001) Bayesian time-domain approach for modal updating using ambient data. Probabilistic Eng Mech 16: 219–231
18. Yuen KV, Katafygiotis LS (2003) Bayesian fast Fourier transform approach for modal updating using ambient data. Adv Struct Eng 6: 81–95
19. Au SK, Zhang FL, Ni YC (2013) Bayesian operational modal analysis: theory, computation, practice. Comput Struct 126:3–14
20. Au SK (2011) Fast Bayesian FFT method for ambient modal identification with separated modes. J Eng Mech 137:214–226
21. Hu YJ, Sun X, Zhu WD, Li HL (2019) Local damage detection of a fan blade under ambient excitation by three-dimensional digital image correlation. Smart Struct Syst 24(5):597–606
22. Hu YJ, Guo WG, Zhu WD, Xu YF (2019) Local damage detection of membranes based on Bayesian operational modal analysis and three-dimensional digital image correlation. Mech Syst Signal Process 131:633–648
23. Jones EMC, Iadicola MA. A good practices guide for digital image correlation. International Digital Image Correlation Society (2018)
24. Vautard R, Ghil M (1989) Singular spectrum analysis in nonlinear dynamics, with applications to paleoclimatic time series. Physica D 35:395–424
25. Allemang RJ (2003) The modal assurance criterion (MAC): twenty years of use and abuse. Sound Vibration 37(8):14–21